

ISTANBUL TECHNICAL UNIVERSITY ★ GRADUATE SCHOOL OF SCIENCE
ENGINEERING AND TECHNOLOGY

**LUBRICATION ANALYSIS
OF CAM AND TAPPET CONTACT**

M.Sc. THESIS

**Özgür GÖÇMEN
(503101718)**

Department of Mechanical Engineering

Automotive Programme

JUNE 2013

ISTANBUL TECHNICAL UNIVERSITY ★ GRADUATE SCHOOL OF SCIENCE
ENGINEERING AND TECHNOLOGY

**LUBRICATION ANALYSIS
OF CAM AND TAPPET CONTACT**

M.Sc. THESIS

**Özgür GÖÇMEN
(503101718)**

Department of Mechanical Engineering

Automotive Programme

Thesis Advisor: Assoc. Prof. Özgen AKALIN

JUNE 2013

İSTANBUL TEKNİK ÜNİVERSİTESİ ★ FEN BİLİMLERİ ENSTİTÜSÜ

**KAM VE SUPAP FİNCANI TEMASININ
YAĞLAMA ANALİZİ**

YÜKSEK LİSANS TEZİ

**Özgür GÖÇMEN
(503101718)**

Makina Mühendisliği Anabilim Dalı

Otomotiv Mühendisliği Programı

Tez Danışmanı: Doc. Dr. Özgen AKALIN

HAZİRAN 2013

Özgür Göçmen, a **M.Sc.** student of **ITU Graduate School of Science Engineering and Technology** student ID **503101718** successfully defended the **thesis** entitled “**LUBRICATION ANALYSIS OF CAM AND TAPPET CONTACT**”, which he prepared after fulfilling the requirements specified in the associated legislations, before the jury whose signatures are below.

Thesis Advisor : **Assoc. Prof. Özgen AKALIN**
İstanbul Technical University

Jury Members : **Asst. Prof. Osman Akın KUTLAR**
İstanbul Technical University

Assoc. Prof. Muammer ÖZKAN
Yıldız Technical University

Date of Submission : 03 May 2013
Date of Defense : 03 June 2013

To my family and nephew,

FOREWORD

I would like to express my sincere appreciation to my advisor, Dr. O. Akalin, for his invaluable guidance and encouragement throughout the course of this work. I would also like to thank Onur Zobi for his helpful support during the model development.

May 2013

Özgür GÖÇMEN

TABLE OF CONTENTS

	<u>Page</u>
FOREWORD	ix
TABLE OF CONTENTS	xi
ABBREVIATIONS	xiii
LIST OF TABLES	xv
LIST OF FIGURES	xvii
SUMMARY	xix
ÖZET	xxi
1. INTRODUCTION	1
1.1 Literature Survey	2
1.2 Scope of Research	6
2. LUBRICATION ANALYSIS OF CAM - TAPPET CONTACT	7
2.1 General Remarks	7
2.1.1 Principle of elastohydrodynamic lubrication	8
2.1.2 Principle of hydrodynamic lubrication	9
2.2 Theory and Modeling	12
2.2.1 Cam surface coordinates	13
2.2.2 Kinematic characteristics of cam profile	14
2.2.2.1 Instantaneous radius of curvature	15
2.2.2.2 The entraining velocity	17
2.2.3 Contact load definition	17
2.2.4 The solution procedure	19
2.2.4.1 Boundary conditions	19
2.2.4.2 Initial conditions	20
2.2.4.3 Numerical procedure	20
3. RESULTS AND DISCUSSION	23
3.1 Input Data Set	23
3.2 Analysis Results	25
3.2.1 Effect of surface kinematics	25
3.2.2 Effect of rotational speed	27
3.2.3 Effect of lubricant viscosity	28
3.2.4 Comparison of classical EHD theory and developed calculation model ..	28
4. CONCLUSIONS	31
REFERENCES	33
CURRICULUM VITAE	35

ABBREVIATIONS

α	: Pressure Coefficient of Viscosity
η	: Lubricant Viscosity
E'	: Combined Elastic Modulus of Two Contacting Surfaces
w	: Load per Unit Contact Width
R	: Combined Radius of Curvature of Two Contacting Surfaces
U	: Hydrodynamic Entraining Velocity
h_T	: Local Film Thickness
h	: Nominal Film Thickness
p	: Local Pressure
δ_1, δ_2	: Surface Roughness Profiles
$\overline{h_T}$: Average Gap
σ	: Composite Surface Roughness
ϕ_x, ϕ_y	: Pressure Flow Factors
c	: Nominal Radial Clearance between Cam and Tappet
R_b	: Base Circle Radius of Cam
ω	: Camshaft Angular Speed
ϕ_c	: Contact Factor
W_P	: Load Carried by Lubricant Film
W_A	: Load Carried by Asperities
θ	: Cam Angle
$y(\theta)$: y Component of the Cam Surface
$s(\theta)$: Displacement of the Follower
$x(\theta)$: Lateral Displacement
$v(\theta)$: Follower Velocity
$R_A, \sigma_A(\theta)$: Polar Coordinates of the Contact Point
$x_s, y_s(\theta)$: Cartesian Coordinates Of the Contact Point
$V_{Q/t}$: Velocity of the Instantaneous Contact Point
j_θ	: Geometric Acceleration
ρ	: Instantaneous Radius of Curvature
F_s	: Total Spring Force
F_{si}	: Installed Spring Force
F_{sp}	: Lift Dependent Polynomial Spring Force
F_i	: Total Inertial Force
m	: Valve Assembly Mass
a	: Acceleration of Mass Center
\dot{H}	: Squeeze Film Velocity
ε	: Convergence Criterion

LIST OF TABLES

	<u>Page</u>
Table3.1 :Input Data.....	23

LIST OF FIGURES

	<u>Page</u>
Figure 1.1 :Valve train mechanisms (AVL Excite TD Users Guide)	1
Figure 2.1 : Stribeck diagram.....	7
Figure 2.2 : Elastohydrodynamic contact between cam and follower (Kreuter and Pischinder, 1985)	8
Figure 2.3 : Film thickness function (Akalın,1999).....	10
Figure 2.4 : Free Body diagram of equivalent calve train system	12
Figure 2.5 : Geometry for derivation of the surface contour of a radial cam with flat- faced follower (Robert and Norton, 2002).....	13
Figure 2.6 : Various cam profile examples	14
Figure 2.7 : An automotive cam profile with its kinematic characteristics	15
Figure 2.8 : Cam to tappet contacFigure 2.10 : Inertial load characteristics t kinematics, Kushwahu (2003)	16
Figure 2.9 : Spring load characteristics.....	18
Figure 2.10 : Inertial load characteristics.....	19
Figure 3.1 :Variation in the radius of curvature	24
Figure 3.2 :Variation in the hydrodynamic velocity	24
Figure 3.3 :Geometrically scaled oil film thickness profile	25
Figure 3.4 :Oil film thickness at the cam – tappet interface	26
Figure 3.5 :Oil film thickness with different engine speeds	27
Figure 3.6 :Oil film thickness with various SAE grade oils	28
Figure 3.7 :Oil film thickness with classical EHD theory and developed model	29

LUBRICATION ANALYSIS OF CAM AND TAPPET CONTACT

SUMMARY

Mainly, there are three different friction loss sources in internal combustion engines, which are valve train system, piston-ring assembly and engine bearings. A significant source of mechanical inefficiency in ICE is the lubricated valvetrain components. In this study, improvement of a computational model for the simulation of cam - tappet lubrication has been investigated using both elastohydrodynamic lubrication theory and mixed lubrication concept. A computational scheme for mixed lubrication concept based on Akalin and Newaz's (1999) model has been adapted for cam - tappet contact. A MATLAB code has been developed to simulate lubrication condition of cam - tappet contact. Program contains two main parts to calculate lubrication parameters within contact zone. To calculate the lubricant film thickness and pressures between the contact surfaces of cam - tappet, average Reynolds equation was solved simultaneously with the initial and boundary conditions for the mixed lubrication regime. Apart from mixed lubricated contact zones, elastohydrodynamic lubrication regime occurs in cam - tappet interaction. Minimum oil film thickness was calculated according to equation Dowson and Higginson formula for the EHD lubrication. Hydrodynamic pressure distribution, asperity contact pressure, lubricant film thickness, load carried by oil film and non-dimensional squeeze film velocity are calculated for each cam angle degree. Variation in the load, the radius of curvature and the hydrodynamic entraining velocity were considered in the analysis. For the hydrodynamic lubrication regime, surface roughness characteristics were taken into account. According to the code algorithm, calculated minimum oil film thickness from Reynolds equation cannot be smaller than Dowson and Higginson formula. Hence, some contact zones were found in hydrodynamic lubrication while some of them were found in EHD lubrication. At the results section, oil film thickness results were examined in terms of lubricant viscosity and rotational speed parameters. Oil film thickness increases with the higher engine speed and lubricant viscosity.

KAM VE SUPAP FİNCANI TEMASININ YAĞLAMA ANALİZİ

ÖZET

İçten yanmalı motorlarda, supap mekanizması, piston segman takımı ve motor yatakları, temel üç farklı sürtünme kaybı kaynağı olarak gösterilebilir. Yağlanan supap mekanizması elemanları, içten yanmalı motorlarda mekanik verimsizliğe sebep olan başlıca etmenlerdendir. İçten yanmalı motorlardaki toplam sürtünme kaybının % 7.5 – 21’lik bir kısmını supap mekanizmasının sürtünme kayıpları oluşturmaktadır. Supap mekanizması dahilinde, kam ve supap fincanı teması önemli bir bölümü oluşturmaktadır. İtici çubuklu supap mekanizmalarında, kam supap fincanı kaynaklı sürtünme kayıpları, toplamın % 85’ini oluşturmakta, direkt etkili supap mekanizmalarında ise neredeyse toplam sürtünme kaybını oluşturmaktadır. Bu çalışmada supap mekanizması elemanlarından, kam ve supap fincanı yağlaması incelenmiş ve yağlama simülasyonu için hesaplamalı bir model geliştirilmiştir. Çalışmanın başında, elasto hidrodinamik ve hidrodinamik yağlama rejimlerinin prensipleri özetlenmiş, analiz algoritmasının temelini oluşturan denklemler çıkarılmıştır. Elasto hidrodinamik yağlama rejimi temelinde, temas yüzeylerinin ince bir film ile birbirinden ayrılmasının haricinde, temas eden yüzeylerin şekil değişimlerinin de etkisi bulunmaktadır. Elasto hidrodinamik yağlama rejimi genel olarak yoğunlaşmış yükleme şekillerinin gerçekleştiği sistemlerde gözlenmektedir. Bunlar yuvarlanmalı yataklar, kam ve itici mekanizmaları ve benzeri sistemlerdir. Hidrodinamik yağlama rejiminde ise birbiri ile temas halinde olan yüzeylerin, oluşan bir yağ filmi tabakası ile birbirlerinden ayrıldığı kabul edilir. Oluşan yağ film profili, yüzey geometrilerindeki farklılıklara, yüzey kinematik özelliklerine ve kullanılan yağ özelliklerine bağlıdır.

Geliştirilen yağlama modeli için hem elasto hidrodinamik yağlama rejimi hem de karma yağlama rejimi göz önünde bulundurulmuştur. Akalin ve Newaz tarafından piston segman takımı için geliştirilmiş karma yağlama rejimi modeli, kam ve supap fincanı teması için adapte edilmiştir. Modelleme sürecinde, supap mekanizmasının tabi olduğu yükler belirlenmiştir. Bu yükler temel olarak, hareketli supap mekanizması parçaları için toplam atalet kuvveti ve valf yayı sıkıştırma kuvvetidir. Supap mekanizmasının çalışması incelendiğinde, kam ve supap fincanı temas yüzeyleri arasında oluşan yağ filmi, toplam atalet ve yay yükünü dengelemektedir. Bu prensip üzerinden modeller kurulmuş ve analizler yakınsatılmaya çalışılmıştır. Kam ve supap fincanı yağlama analizi için MATLAB programı kullanılarak bir simülasyon kodu yazılmıştır. Program temel olarak iki kısımdan oluşmaktadır. Kam ve supap fincanı yüzeyleri arasındaki yağ film kalınlığını hesaplamak için ortalama Reynolds denklemi dönüş açısına bağlı olarak anlık şekilde çözümlenmiştir. Karma yağlama rejimi için, yağ film kalınlığı çözümü, ilgili başlangıç ve sınır koşulları denklemlerde kullanılarak sağlanmıştır. Analiz girdisi olarak, ilk aşamada kam geometrisi kullanılmıştır. Verilen kam yükseltme eğrisi kullanılarak, yüzey koordinatları hesaplanmış, bu veriler ışığında da temas noktasındaki akışkan giriş hızı anlık olarak hesaplanmıştır. Yüzey akış ve temas faktörleri Akalin’ın

alışmasından alınmış ve analizlere girdi olarak kullanılmıştır. Program girdileri ile analizler gerçekleştirilmiş, yük dengesini esas alan yakınsama kriteri kullanılarak temas yüzeyleri arası basın dağılımı elde edilmiştir. Karma yağlama rejiminin hesaplandığı bölgeler haricinde, kam ve supap fincanı temasında elasto hidrodinamik yağlama rejimi gözlenmiştir. Elasto hidrodinamik rejimin baskın olduğu kimi temas açılarında, minimum yağ film kalınlığı Dowson ve Higginson tarafından geliştirilmiş formülasyon kullanılarak hesaplanmıştır. Bu çözüm algoritmasında, toplam atalet kuvveti ve toplam yay yükü her bir kam açısı için hesaplanmış ve analiz girdisi olarak kullanılmıştır. Bunun yanı sıra yine her bir kam açısı için, yüzey temas noktasında eğrilik yarıapı ve akışkan giriş hızları hesaplanmış, yağ filmi kalınlığı hesabı için girdi olarak kullanılmışlardır. Hidrodinamik ve pürüzlülük teması basın dağılımları, yağ film kalınlıkları, oluşan yağ filmi tarafından taşınan yük ve boyutsuz yağ filmi sıkışma hızı her bir kam mili dönüş açısı için hesaplanmıştır. Sistem üzerine uygulanan yükteki deęişim, kam üzerindeki eğrilik yarıapındaki deęişim ve hidrodinamik giriş hızındaki deęişim, hesaplar yapılırken göz önünde bulundurulmuşlardır. Hidrodinamik yağlama rejimi için yüzey pürüzlülük profilleri ayrıca hesaplamalara katılmıştır. Geliştirilen kod algoritmasına göre, Reynolds eşitliği kullanılarak hesaplanan minimum yağ filmi kalınlığı, Dowson ve Higginson'un geliştirdiği formül kullanılarak hesaplanan yağ film kalınlığından daha düşük bir deęerde olması engellenmiştir. Bu sayede kam profili üzerinde, bazı bölgeler hidrodinamik yağlama rejimine sahip görülürken, bazı bölgeler ise elasto hidrodinamik yağlama rejimine sahip olacak şekilde hesaplar gerçekleştirilmiştir. Çalışmanın sonuç bölümünde, yağ film kalınlıkları, deęişken yağ viskoziteleri ve farklı motor çalışma hızları açısından incelenmiştir. Artan yağ viskozitesi ve motor hızı ile birlikte yağ film kalınlıklarının da arttığı gözlenmiştir. Sonuçlar ayrıca kam yüzeyi kinematığı açısından incelenmiş ve yüzey profili üç kısma ayrılarak sonuç deęerlendirmeleri yapılmıştır. Buna göre; kam profilinin temel daire bölümünde, durağan yağ filmi kalınlığı tespit edilmiştir. Eğrilik yarıapı ve temel daire boyunca yağ giriş hızı sabit olduğu için, hesaplanan film kalınlığı da sabit olmuştur. Buna rağmen kam yan yüzey geçişindeki ufak film kalınlığı artışları, yine o bölgelerdeki artan yağ giriş hızları ile açıklanabilmektedir. Yine de temel daire bölümünde, düşük eğrilik yarıapı ve düşük giriş hızları sebebiyle elasto hidrodinamik yağlama rejimi baskın olarak gözlenmiştir. Kam profilinin her iki yan tarafı için, bölgede hidrodinamik yağ filmi oluşumu gözlenmiştir. Yüksek eğrilik apı ve yağ giriş hızları sebebiyle ortalama Reynolds denklemi çözülebilmiş ve bölgedeki basın dağılımı elde edilmiştir. Bunun yanı sıra bölgede pürüzlülük basınları da saptandığı için, bu kısım ise karışık yağlama rejiminin gerçekleştiği söylenmiştir. Son bölüm ise kam ucu olarak adlandırılmıştır. Çok düşük eğrilik yarıapı ve neredeyse 0'a yakın yağ giriş hızları sebebiyle, bölgedeki yağlama rejimi tekrardan elasto hidrodinamik olarak adlandırılmıştır. Yapılan çalışma ile kam supap fincanı teması yağlama performansını deęerlendirebilecek yeni bir yöntem ortaya konmuştur. Geliştirilen yöntem ile hem elasto hidrodinamik hem de karma yağlama rejimleri bir arada ele alınmıştır. Yük deęişimleri, eğrilik yarıapı ve akışkan giriş hızı deęişimleri göz önünde bulundurulmuştur. Geliştirilen simülasyon aracı ile her çeşit kam supap fincanı tasarımı, yağlama özellikleri açısından incelenebilir hale gelmiştir. Kullanılan akışkanın özellikleri ve ilgili temas yüzeylerinin malzeme özellikleri de geliştirilen model içerisinde etkileri gözlenebilir parametreler olarak tanımlanmıştır. Bu sayede kurulan model ile karmaşık yapıdaki kam supap fincanı dinamikleri incelenebilir yorumlanabilir duruma getirilmiştir. Son olarak, yapılan çalışmayı ilerletmek, genişletmek adına bir kaç hususa değinilmiştir. Bunlardan ilki, elasto hidrodinamik

rejime sahip bölgelerde, kam açısına bağlı anlık çözümlerin yapılabileceği şekilde kurulan algoritmanın genişletilebilmesidir. İkinci olarak modele, kam taç yarıçapı ve koniklik açısı gibi parametrelerin de eklenmesi ile yağlama analizi performansı artırılabilir. Bunların yanı sıra, sürtünme katsayısı belirlenmesi ve aşınma mekanizmalarının eklenmesi çalışmanın gelecekteki aşamalarından bazıları olarak gösterilebilir.

1. INTRODUCTION

Mainly, there are three different friction loss sources in internal combustion engines, which are valve train system, piston-ring assembly and engine bearings. A significant source of mechanical inefficiency in ICE is the lubricated valvetrain components. The friction losses of the valvetrain components represent about 7.5-21 percent of total friction losses in ICE (Messe et al, 1999). One of the most critical parts is the cam - tappet interaction. Cam - tappet friction losses account about 85 percent of the total friction losses in push rod valve trains and almost the total friction losses in direct acting valve mechanism (Teodorescu et al, 2002). Figure 1.1 illustrates two different valve train systems; direct acting valve train and push rod valve train.

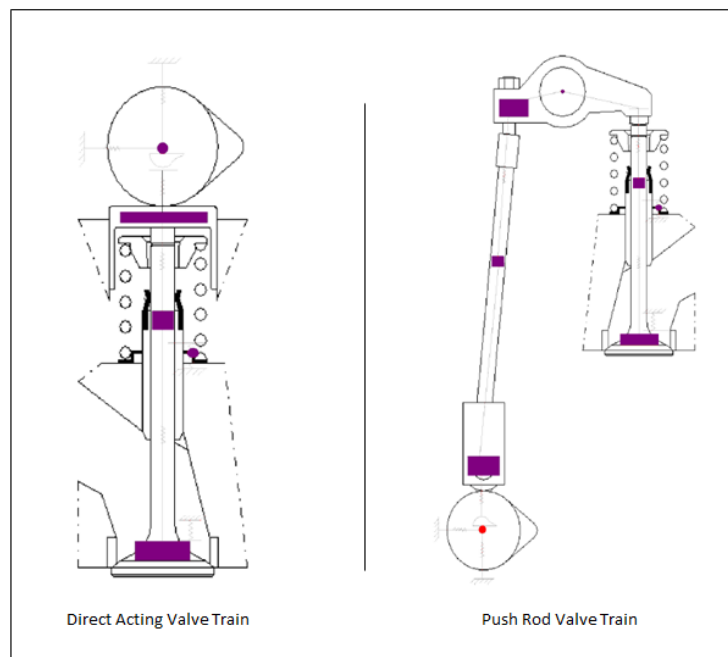


Figure 1.1 : Valve train mechanisms (AVL Excite TD Users Guide)

Since the cam - tappet contact is subjected to continuous variation of load, speed, geometry and dynamic effects of the valvetrain system, it is critical to understand what occurs inside a cam-follower contact (Vela et al, 2010). The motivation behind this study is to understand complex phenomena between cam and tappet contact.

1.1 Literature Survey

Lee (1971) has developed a transient solutions for elastohydrodynamic lubrication. In the study, both transient Reynolds equation and the elasticity equation are solved. It is stated that velocity plays an important role for the solutions since it causes the lubricant to be entrapped within the contact region. A relation between an asperity and lubricant in terms of pressure and lubricant film thickness was found. It was shown that surface asperities have a significant effect in generating a continuous fluid film in the contact zone.

Dowson and Higginson (1977) have developed a full numerical solutions, including a wide range of lubrication conditions. An oil film thickness formula which was used by several authors in order to calculate oil film thickness at EHD contacts were derived.

Kreuter and Pischinger (1985) have developed a mathematical model to describe the dynamic behaviour of valve train system. In the study, they have modeled the oil film between cam and follower and investigated the lubrication conditions in the contact area of cam and follower. The surface speed between and the normal movement between cam and follower are the main parameters that affect the existing thickness of the oil film. They used the Dowson and Higginson formula in order to compute oil film thickness and performed an experimental study to measure oil film thickness between cam and follower. Their results showed that there is a good correlation between the calculated values and measured oil film shape.

Lubrecht (1987) has investigated elastohydrodynamic lubrication in terms of line and point contact. In the study, first aim was the calculation of film thickness in lubricated line and point contacts under various loads. In order to investigate the influence of surface roughness, the point contact problem was solved, using many calculation points. In the research, elastohydrodynamic lubrication governing equations were derived. Reynolds equation was solved with the following assumptions; isothermal and pure viscous fluid flow, without internal and external forces, time dependency only through boundary equations and narrow gap assumption. The elastic equations were solved both line and point contact conditions. Barus and Roelands viscosity - pressure relations were used in his study. As a density – pressure relation, Dowson and Higginson formula was used. The multigrid

technique was developed for the numerical solution of elastohydrodynamic lubrication field. The main role of the multigrid technique is not to reduce error, but to smooth it out. Thus, convergence is faster and the work involved is much smaller.

Chang (1988) has developed a multi level computational algorithm that can efficiently and accurately solve both steady-state and transient EHD line contact problems. The calculation model also simulates the processes of micro-EHD lubrication associated with surface irregularities. It is reported that the simulation results show good correlation with previous experimental results. Chang also investigated the effects of lubricant rheology on the film thickness and pressure in micro-EHD lubrication. It is indicated that, under simple sliding conditions, the local pressure generation and surface deformation depend on the lubricant rheology. Surface kinematic conditions, especially the time dependent term $\partial h / \partial t$, can significantly change the local pressure generation.

Gecim (1992) has studied the lubricant film thickness and Hertzian pressures at the cam - tappet contact. In order to find EHD film thickness lubrication regimes chart was used with the thermal and squeeze-film effects considerations. Thermal correction factor was used in order to find the corrected film thickness. Besides the elastohydrodynamic contact analysis, a mixed friction model was integrated into the analysis. The aim was to predict the respective contributions from hydrodynamic and boundary lubrication to overall friction at the cam - tappet contact zone. The model was based on Greenwood and Tripp. Gecim also included a model of tappet spin allowing for slip at the contact area. At the results section of the study, the overall coefficient of friction, surface flash temperatures, effects of lubricant types, surface roughness and tappet spin were reported. With the knowledge of influential parameters which are tappet-foot radius, cam-taper angle and tappet-crown radius, the optimization possibility of the cam - tappet contact for lower friction loss was indicated. In addition to the calculations, the results are compared with the experimental data.

Jiang et al. (1999) has an investigation regarding a mixed elastohydrodynamic lubrication model with asperity contact. Their model deals with EHL problem in the very thin lubricant film zone where the film is not thick enough to separate contacting surfaces. They used the Reynold equations only in the lubricated area. In the asperity contact zone, asperity pressure is calculated by the interaction of two

mating surfaces. As a result, total applied load is carried out by the lubricant film and the asperities. They introduced the load ratio, contact area ratio and average gap to characterize the performance of mixed lubrication with asperity contacts. They also reported the asperity orientation and the effect of rolling-sliding condition.

Kushwaha et al. (2000) have been conducted an analysis non-linear constrained valve train system. They showed the simultaneous solution of the Lagrangian dynamics for the system, together with an approximate quasi-static elastohydrodynamic solution of the lubricated contact. They used an extrapolated oil film thickness formula which includes both entraining and squeeze film effects. They examined the effect of spring surge on the contact separation and residual vibrations of the system. They also investigated the lubricant pressure distribution and film thickness, including during start-up and acceleration.

Messe and Lubrecht (2000) have performed a transient elastohydrodynamic analysis of a cam - tappet contact. They used multi-grid, multi-level and multi-integration techniques to reduce the computing time. Their model includes the variations in the radius of curvature of the cam, the variations in the hydrodynamic velocity and the variation in the load. They indicate that the variation in the radius of curvature is dependent on the cam geometry. Radius of curvature is defined as a function of cam rotational angle. They found a relation between the entrainment velocity and the displacement of the contact point. They described the variation in the load as a function of the stiffness of the spring and the inertial forces and consequently of angular velocity. They reported their results for the different zones of the cam. According to their study, both elastohydrodynamic and hydrodynamic lubrication regimes have been observed. They also reported the importance of squeeze effect on the oil film around cam nose contact.

Glovnea and Spikes (2001) investigated the influence of cam follower motion on elastohydrodynamic film thickness. They indicate that at some points in the cam cycle event, the entrainment velocity and theoretical steady state film thickness becomes zero. Since the possible acceleration or squeeze effects did not consider in steady state solutions, they intended to test the validity of this approximation. They simulated cam-follower kinematic cycles in a model ball on disc. The results showed that squeeze effects play an important role in the lubrication of this type of

mechanism. They also reported that a finite lubricant film was retained even in the positions where the entrainment speed was zero.

Teodorescu and Tazara (2003) have an investigation regarding the simplified elastohydrodynamic friction model of the cam - tappet contact. In this study, they analyzed the contact conditions between cam and a flat tappet in order to develop a method for the calculation of the friction force. They used Greenwood and Tripp's model for the contact of two rough surfaces. They argued that oil film thickness has not a significant effect on the friction force when non-Newtonian behavior of the oil is dominant. They also reported the followings; There is a poor influence of the load on the oil film thickness in EHD lubrication, oil viscosity and entrainment speed are the main parameters that affect the oil film thickness, Hertzian pressure distribution is observed in the contact region, excepting the oil exit, the oil film is parallel in the contact region and there is always oil film retained in EHD lubrication, even at the reversal of the entrainment speed. At the end of their study their simplified friction model was experimentally validated by their single cylinder diesel engine experimental setup. They developed an original technique to allow the measurement of the friction forces on the tappet. They used an equipped tappet which can measure forces and moments applied on the tappet. With this measurement technique, they also evaluated the friction force on cam-tappet and tappet-bore to determine the angular rotation of the tappet.

Teodorescu and Taraza (2004) have an other study regarding the cam - tappet contact condition. They investigated the tribological contact conditions between a polynomial automotive cam and a flat follower. They used a multi body model of the system to represent the complex tappet motions. They examine both cam-tappet and tappet-tappet bore lubrication conditions. They reported that at high engine speeds the boundary friction is observed at the closing event of the cam and hydrodynamic and mixed lubrication is observed at the opening event of cam.

Zhu (2007) studied some aspects of numerical solutions of thin-film and mixed elastohydrodynamic lubrication. He states that in elastohydrodynamic region, converged and accurate numerical solutions become difficult. In his study, he conducted analyses with various computational meshes, various cut-off values for handling contact, on different levels of central film thickness. As a result of his

studies, he indicated that the computational mesh density plays significant role on the EHD film thickness when the lubricant film is very thin.

Roshan et al. (2009) evaluated frictional losses in a direct attack valve train through the use of tribofilm friction performance model in boundary and mixed lubrication conditions. They included mixed lubrication concept based on a transition model. They assumed that the lubrication regimes ranges from EHD through mixed to boundary lubrication is to be isothermal and full separation of the sliding surfaces is not guaranteed. In the study, they also included the chemical sensitivity of the additives used in automotive lubricants by using a typical friction modifier. With the combination of elastohydrodynamic and mixed lubrication model, their friction torque predictions showed good correlation with the experimental data from motored cylinder head of a typical direct attack design.

Vela et al. (2011) have an investigation on cam follower contacts. In their study, they modified the existing experimental apparatus to measure oil film thickness and friction force between cam and follower. Besides the experimental study, they also conducted theoretical simulations in order to interpret on the experimental results.

1.2 Scope of Research

In this study, computational model for the simulation of cam - tappet lubrication has been improved considering both elastohydrodynamic lubrication theory and mixed lubrication concepts. A computational scheme for mixed lubrication concept based on Akalin and Newaz's (1999) model has been adapted for cam - tappet contact.

2. LUBRICATION ANALYSIS OF CAM - TAPPET CONTACT

2.1 General Remarks

There are three types of lubrication occur in valvetrain components: full-film, mixed film and boundary lubrication. In full film lubrication condition, two contacting surfaces are fully separated by a lubricant. In boundary lubrication condition, two contacting surfaces are physically in contact because of geometry of surfaces, excessive load, surface roughness or lack of sufficient lubricant. In mixed film lubrication regime, two contacting surfaces face with both lubrication film and asperity contact. Figure 2.1 shows three different lubrication regimes in terms of Sommerfeld number and friction quantities.

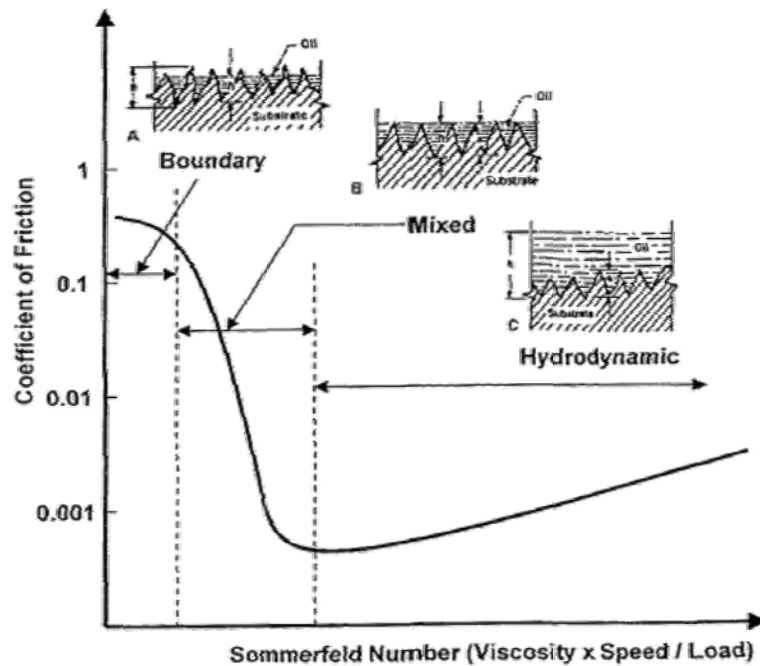


Figure 2.1 : Stribeck diagram

In this study, mixed film, hydrodynamic and elastohydrodynamic lubrication regimes are introduced without presentation of complete derivations of the governing equations since this is out of scope of study.

2.1.1 Principle of elastohydrodynamic lubrication

Elastohydrodynamic lubrication is a type of lubrication that includes the elastic deformation of the lubricated surfaces. In EHD lubrication, the contact surfaces are not only separated by a thin lubricating film, but also elastically deformed to an amount comparable to the film thickness (Chang, 1988). EHD lubrication can be seen under concentrated load supporting contacts such as rolling bearings, cam follower systems etc. Typical shape of elastohydrodynamic contact between cam and follower can be seen at Figure 2.2.

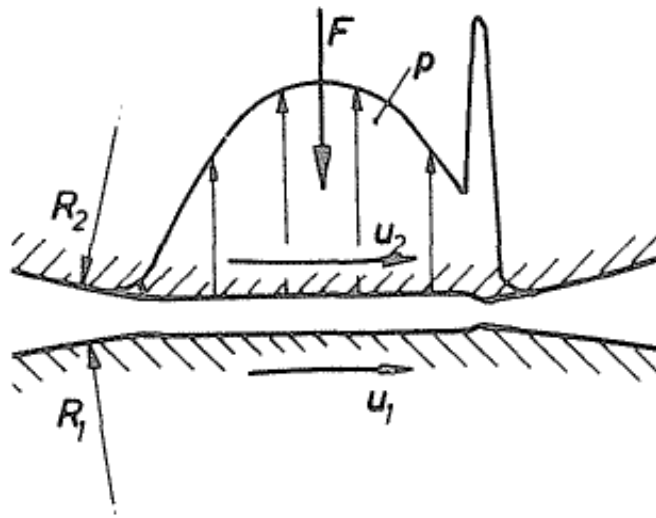


Figure 2.2 : Elastohydrodynamic contact between cam and follower (Kreuter and Pischinder, 1985)

There are large numbers of studies regarding to numerical solution of elastohydrodynamic lubrication. These investigations include the deformation behavior of the surfaces, hydrodynamic pressure generation in the fluid and non-linear viscosity –pressure relation of the lubricant.

An extensive study is performed by Dowson and Higginson (1966). They have developed a formula based on the results of their numerical computations, in order to calculate the thickness of the elastohydrodynamic oil film.

$$h_{EHD} = 1.6 * \alpha^{0.6} * \eta^{0.7} * (E')^{0.03} * w^{-0.13} * R^{0.43} * \left| \frac{U}{2} \right|^{0.7} \quad (2.1)$$

where,

α = Pressure coefficient of viscosity

η = Oil viscosity at the temperature of the surfaces and at atmospheric pressure

E' = Combined Elastic Modulus of two contacting surfaces

w = Load per unit contact width

R = Combined radius of curvature of two contacting surfaces

U = Hydrodynamic entraining velocity

This equation considers Hertzian deformations in the contact area as well as the pressure dependence of the lubricant viscosity (Kreuter and Pischinder, 1985).

2.1.2 Principle of hydrodynamic lubrication

In hydrodynamic lubrication, generation of a hydrodynamic pressure in the lubricant provides the lubrication between two surfaces. The generation of hydrodynamic pressure depends on the contact geometrical configuration, surface kinematic conditions and the lubricant properties (Chang, 1988). For an isothermal and incompressible lubricant, the pressure in hydrodynamic contacts is governed by the Reynolds equation.

$$\frac{\partial}{\partial x} \left(\frac{h^3}{12\eta} \frac{\partial p}{\partial x} \right) + \frac{\partial}{\partial y} \left(\frac{h^3}{12\eta} \frac{\partial p}{\partial y} \right) = \frac{U_1 + U_2}{2} \frac{\partial h_T}{\partial x} + \frac{\partial h_T}{\partial t} \quad (2.2)$$

where, h_T is local film thickness, h is the nominal film thickness, p is local pressure and η is viscosity of lubricant. The local film thickness is defined as,

$$h_T = h + \delta_1 + \delta_2 \quad (2.3)$$

where, δ_1 and δ_2 are surface roughness profiles of the surfaces that can be seen Figure 2.2.

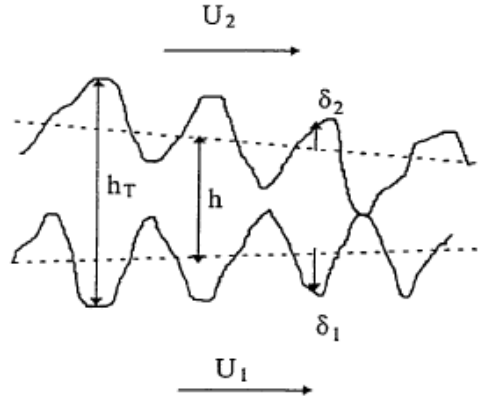


Figure 2.3 : Film thickness function (Akalin,1999)

Patir and Cheng (1978) modified this equation in order to include surface roughness on partial hydrodynamic lubrication. This approach is based on Average Reynolds equation in terms of pressure and shear flow factors, which are functions of surface roughness characteristics.

$$\frac{\partial}{\partial x} \left(\phi_x \frac{h^3}{12\eta} \frac{\partial \bar{p}}{\partial x} \right) + \frac{\partial}{\partial y} \left(\phi_y \frac{h^3}{12\eta} \frac{\partial \bar{p}}{\partial y} \right) = \frac{U_1 + U_2}{2} \frac{\partial h_T}{\partial x} + \frac{U_1 - U_2}{2} \sigma \frac{\partial \phi_x}{\partial x} + \frac{\partial \bar{h}_T}{\partial t} \quad (2.4)$$

Here, \bar{h}_T is average gap, σ is composite surface roughness, U_1 and U_2 are the surface velocities. ϕ_x and ϕ_y are pressure flow factors. Patir and Cheng (1978, 1979) have developed a formula in order to calculate flow factors as a function of lubricant film thickness to composite surface roughness ratio and surface roughness orientation. Necessary empirical equations and coefficients to calculate surface flow factors are taken from Akalin's study (1999).

Simplified form of Average Reynolds equation for cam-tappet contacts, where $U_1 = U$ and $U_2 = 0$ can be written as,

$$\frac{d}{dx} \left(\phi_x h^3 \frac{d\bar{p}}{dx} \right) = 6\eta U \left(\frac{d\bar{h}_T}{dx} + \sigma \frac{d\phi_s}{dx} \right) + 12\eta \frac{\partial \bar{h}_T}{\partial t} \quad (2.5)$$

The following non-dimensional parameters are used as in Hu (1994),

$$X = \frac{2x}{b} \quad H = \frac{h}{c} \quad T = t * \omega \quad U^* = \frac{U}{r\omega}$$

$$P = \bar{p} \frac{c^2}{3\eta r \omega b} \quad \sigma^* = \frac{\sigma}{c} \quad \phi_c = \frac{\partial \bar{h}_T}{\partial h}$$

where,

c = Nominal radial clearance between cam and tappet

r = Base circle radius of cam

ω = Camshaft angular speed

$\beta = b/r$

Wu and Zheng (1989) introduced a contact factor ϕ_c in order to reduce numerical work to calculate average separation in the average Reynolds equation. Non-dimensional modified Reynolds equation can be written as,

$$\frac{d}{dX} \left(\phi_x H^3 \frac{dP}{dX} \right) = U^* \left(\phi_c \frac{dH}{dX} + \sigma^* \frac{d\phi_s}{dX} \right) + \beta \phi_c \frac{\partial H}{\partial T} \quad (2.6)$$

By solving Equation 2.5, pressure distribution between cam and tappet contact zone is obtained. Load carried by lubricant film can be calculated integrating the pressure distribution within the effective lubrication length.

$$W_P = \int_{-1}^1 P(X, T) \Psi(P) dX \quad (2.7)$$

where,

$$\Psi(P) \begin{cases} 1, P > 0 \\ 0, P \leq 0 \end{cases}$$

As Reynolds boundary conditions do not allow negative pressure within contact length, positive lubricant pressures have been taken in the force balance.

Contact load for a unit segment $W_A(T)$ is calculated by using Greenwood and Tripp's (1971) asperity contact model as a function of separation of the surfaces.

Total force, which is acting to the cam, is balanced by summation of the asperity and hydrodynamic loads.

$$W_T = W_P(T, H, \dot{H}) + W_A(T, H) \quad (2.8)$$

2.2 Theory and Modeling

Valve train system is subjected to variable spring and inertial forces during cam event cycle. Since there is lubricant between cam lobe and the dynamic part of valvetrain system, total inertial and valve spring forces are balanced with the hydrodynamic and asperity loads between cam and tappet. Figure 2.3 is the free body diagram of equivalent valve train system.

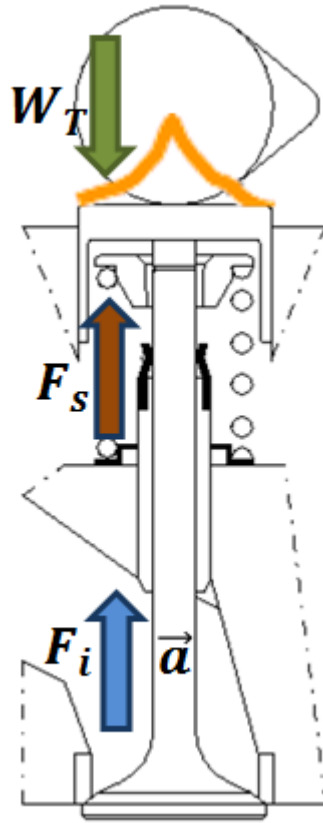


Figure 2.4 : Free Body diagram of equivalent valve train system

2.2.1 Cam surface coordinates

Figure 2.4 shows the geometry of a translating flat-faced follower and cam in two positions, the initial position at $\theta = 0$ and an inverted position at an arbitrary value of cam angle θ .

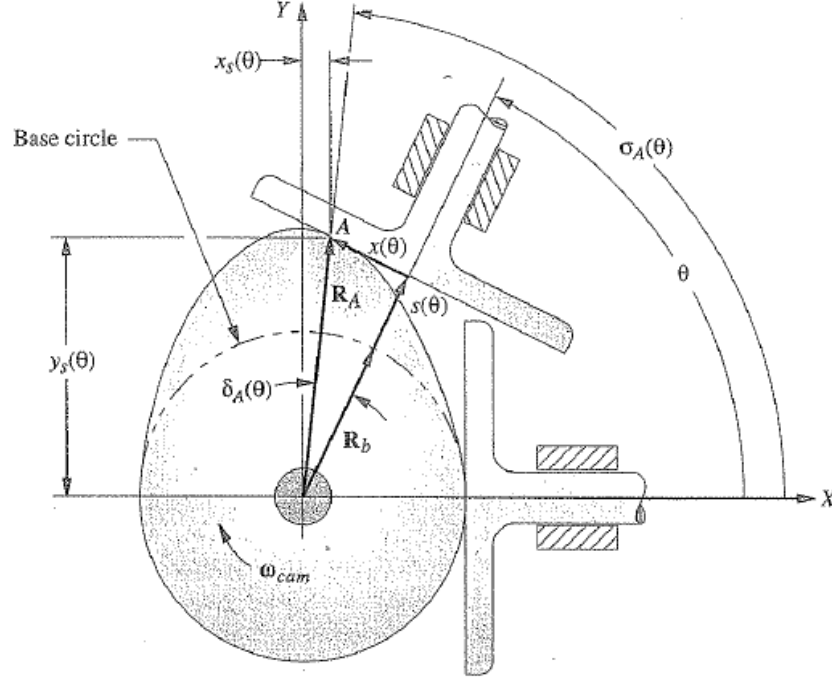


Figure 2.5 : Geometry for derivation of the surface contour of a radial cam with flat-faced follower (Robert and Norton, 2002)

Norton (2002) derived the cam surface coordinates as follows,

$$y(\theta) = R_b + s(\theta) \quad (2.9)$$

where, $y(\theta)$ is the y component of the cam surface contour for any cam angle θ , R_b is the base circle radius and $s(\theta)$ is the displacement of the follower.

The lateral displacement $x(\theta)$ can be defined as,

$$x(\theta) = \frac{V(\theta)}{\omega} = v(\theta) \quad (2.10)$$

where, $v(\theta)$ is the follower velocity.

The polar coordinates of the contact point A for any θ are,

$$R_A(\theta) = \sqrt{[R_b + s(\theta)]^2 + [x(\theta)]^2} \quad (2.11)$$

$$\sigma_A(\theta) = \theta + \tan^{-1} \left(\frac{x(\theta)}{R_b + s(\theta)} \right) \quad (2.12)$$

The Cartesian coordinates of the contact point are then,

$$x_s(\theta) = [R_A(\theta)] \cos [\sigma(\theta)] \quad (2.13)$$

$$y_s(\theta) = -\text{sgn}(\omega)[R_A(\theta)] \sin [\sigma(\theta)] \quad (2.14)$$

where, the *sgn* function accounts for cam rotation direction.

2.2.2 Kinematic characteristics of cam profile

Under ideal conditions, the cam should remain in contact with the tappet at all times; otherwise, the loss of lubricant may ensue. However, owing to the dynamics of the system involved, this may not be the case (Kushwahu et al., 2003). Hence, it becomes important to understand the kinematics of the cam geometrical profile.

At Figure 2.5, various cam profiles that are used in internal combustion engines can be seen.

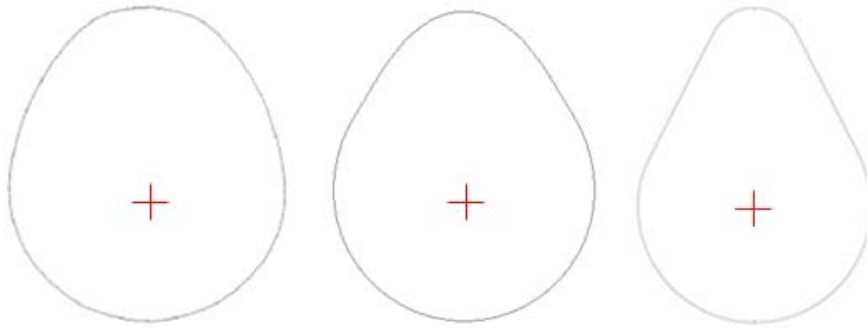


Figure 2.6 : Various cam profile examples

Many cam profiles can be designed for various machines and applications. An example that was used in the analysis is illustrated at Figure 2.6.

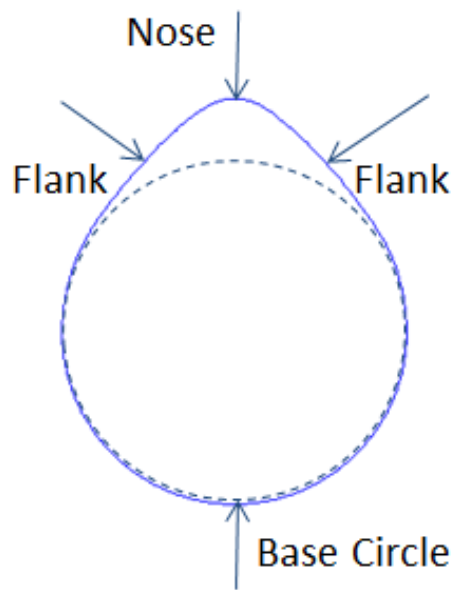


Figure 2.7 : An automotive cam profile with its kinematic characteristics

Given cam profile can be characterized by three different zones; Base Circle, Flank, Nose.

The Base Circle zone: The valve is closed by the spring at base circle zone. Applied load, radius of curvature and the entraining velocity are constant. The conditions are stationary.

The Flank zone: The valve is opened at flank zone. Applied load depends on the inertia and spring loads. Radius of curvature and entraining velocity reach maximum value at the middle of the flank zone.

The Nose zone: Maximum valve lift is occurred at the middle of nose region. Minimum radius of curvature is also seen at the cam nose zone.

2.2.2.1 Instantaneous radius of curvature

Instantaneous radius of curvature is dependent on the cam design and the kinematic characteristics of cam - tappet contact. Due to the cam profile changes during cam event cycle, radius of curvature also changes with the cam rotation angle.

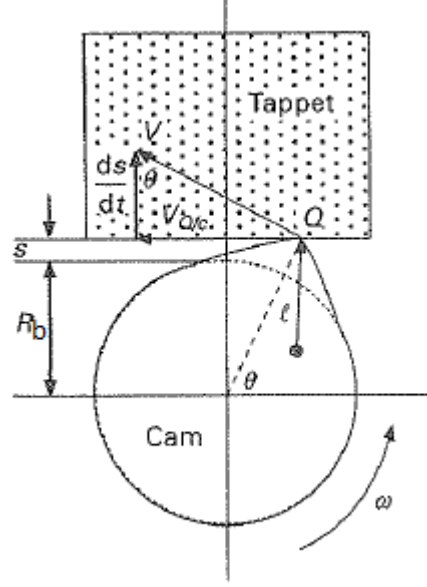


Figure 2.8 : Cam to tappet contact kinematics, Kushwahu (2003)

Figure 2.7 shows the kinematic relation between cam and flat tappet. Kushwahu (2003) derived the instantaneous radius of curvature as follows,

When the rotation of the tappet is ignored, the velocity of the instantaneous contact point Q can be defined as,

$$V_{Q/t} = -\omega j_\theta \quad (2.15)$$

where j_θ is referred to as the geometric acceleration of the tappet caused by the change in the cam profile.

$$j_\theta = \frac{d^2 s}{d\theta^2} \quad (2.16)$$

with the assumption of constant camshaft angular velocity ω , then $\theta = \omega t$. By substituting θ in the above equation,

$$j_\theta = \frac{d^2 s}{d(\omega t)^2} = \frac{1}{\omega^2} \frac{d^2 s}{dt^2} \quad (2.17)$$

The velocity of the contact point Q can also be represented in terms of the instantaneous radius of curvature of the cam profile at the point of contact.

$$V_{Q/c} = V \sin \theta - \omega \rho \quad (2.18)$$

where,

$$V \sin \theta = \omega(R_b + s) \quad (2.19)$$

Since no slip condition is assumed between cam and tappet, equation (2.17) equals equation (2.14). Hence,

$$\omega(R_b + s) - \omega \rho = -\omega j_\theta \quad (2.20)$$

Therefore, the instantaneous radius of curvature at the point of contact is obtained as,

$$\rho = R_b + s + j_\theta \quad (2.21)$$

where R_b is the base circle radius.

2.2.2.2 The entraining velocity

The entraining velocity depends on the contact surface velocities. Kushwaha (2003) states that the entraining velocity U is the average of the surface velocities of the tappet and the cam at the point of contact. Hence,

$$U = \frac{1}{2}(\omega j_\theta + \omega \rho) \quad (2.22)$$

Replacing ρ into equation above gives,

$$U = \frac{1}{2}[\omega j_\theta + \omega(R_b + s + j_\theta)] \quad (2.23)$$

$$U = \frac{1}{2}\omega(R_o + s + 2j_\theta) \quad (2.24)$$

2.2.3 Contact load definition

For cam - tappet mechanism, the applied load W_T is the summation of inertial force from valvetrain assembly and the valve spring load.

Spring Load

Figure 2.8 shows typical load characteristics of automotive valve springs.

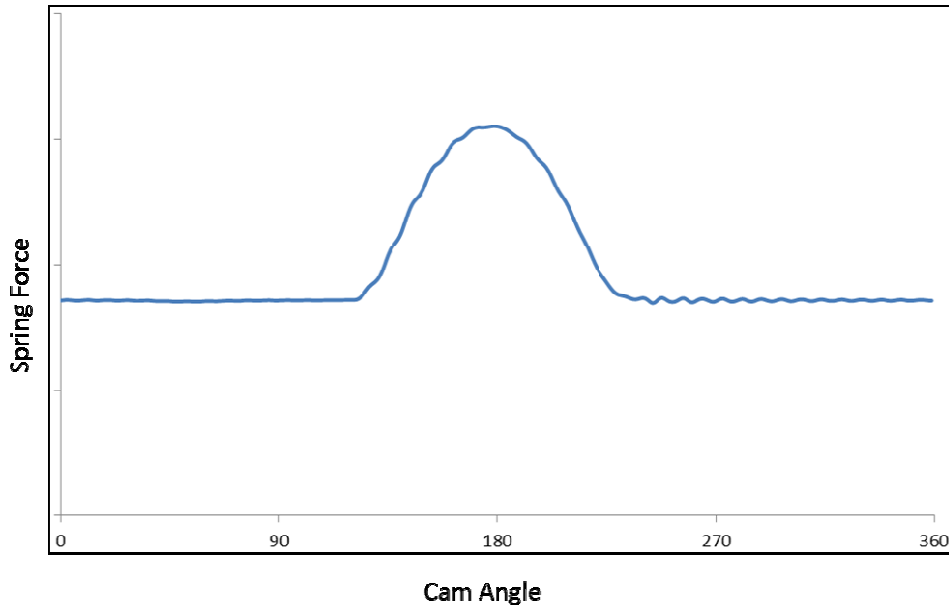


Figure 2.9 : Spring load characteristics

The spring force characteristics are defined by polynomial shape. Total spring force is the summation of installed spring force and lift dependent polynomial spring force

(2.25)

Inertial Load

Newton's second law states that magnitude of the applied force is equal to the time rate of change of momentum of a body. When mass is constant mass and is the acceleration of mass center, total force that is acting at the mass center can be defined as,

(2.26)

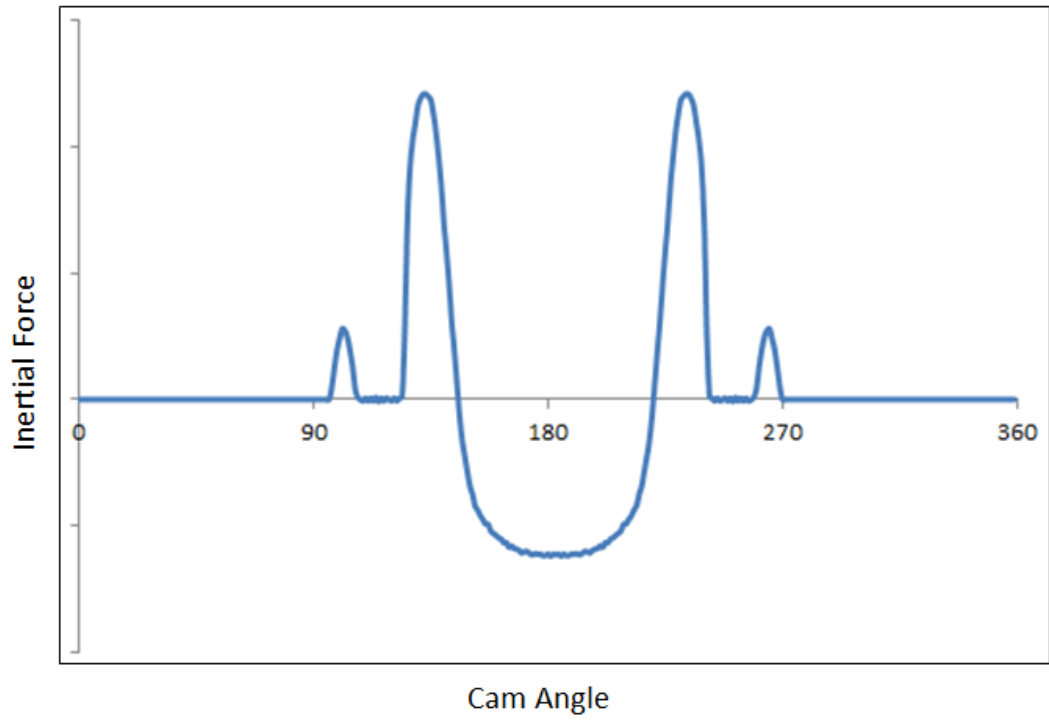


Figure 2.10 : Inertial load characteristics

Figure 2.9 illustrates typical characteristics of inertial load. With the definition of spring and inertial loads, total force acting to the cam can be defined as,

$$W_T = F_s + F_i \quad (2.27)$$

2.2.4 The solution procedure

To calculate the lubricant film thickness and pressures between the contact surfaces of cam - tappet, equation (2.6) is solved simultaneously with the initial and boundary conditions for the mixed lubrication regime. Apart from mixed lubricated contact zones, elastohydrodynamic lubrication regime occurs in cam - tappet interaction. Minimum oil film thickness is calculated according to equation (2.1) for the EHD lubrication.

2.2.4.1 Boundary conditions

There are two boundary conditions applied to the solution, one of them is the ambient pressure assumption at the edges of computational zone. The second one is the Reynolds cavitation boundary condition. Pressure gradient at the cavitation

boundary is zero and the pressure is equal to the atmospheric pressure at the outlet of lubrication regime (Akalın, 1999).

2.2.4.2 Initial conditions

To resolve for the pressure distribution and oil film thickness within contact length, minimum oil film thickness and squeeze film velocity assumptions are used as initial conditions.

2.2.4.3 Numerical procedure

A MATLAB code has been developed to simulate lubrication condition of cam - tappet contact. Program contains two main parts to calculate lubrication parameters within contact zone. For Elastohydrodynamic lubrication regime, Dowson and Higginson formula and for Hydrodynamic lubrication regime, averaged Reynolds equation was used to determine oil film thickness.

To solve Averaged Reynolds equation, the simulation starts with the geometric input definition. For a known cam lift curve, cam surfaces coordinates are derived by using equations (2.12) and (2.13). Cam - tappet contact surfaces are defined for every cam angle by a subroutine and used as an input in the simulation. By using cam lift curve, entraining velocity at the point of contact is calculated according to equation (2.23). Entraining velocity is also given as an input to the program for every solution angle. Surface and shear flow factors (Patir and Cheng, 1978, 1979) and contact factor (Wu and Zheng 1989) are taken from Akalın's study (1999). They are calculated by subroutines and used as an input in the simulation. Using these inputs and assumed initial and boundary conditions, pressure distribution along the contact length is calculated using equation (2.6). Integrating the pressure curve within the effective contact length, the load carried by the lubricant film is calculated. Load carried by surface asperities is also calculated using Greenwood and Tripp's (1971) model.

The convergence criterion is used as Akalın's algorithm (1999). If the load balance in equation (2.8) is not satisfied for the assumed squeeze film velocity, initial squeeze film velocity is modified,

$$\dot{H} = \dot{H} + \Delta \dot{H} \quad (2.28)$$

and solution is repeated until the load balance is satisfied. When the load balance $\varepsilon < \varepsilon_1$ is satisfied where,

ε_1 = Convergence Criterion

and

$$\varepsilon = \left| \frac{W_T - (W_A + W_P)}{W_T} \right| \quad (2.29)$$

calculated squeeze film velocity is used to calculate the new lubricant film thickness. Forward Euler method is used to calculate the lubricant film thickness for the next cam angle.

$$H_{T+\Delta T} = H_T + H \dot{\Delta T} \quad (2.30)$$

Pressure distribution and asperity contact pressure, lubricant film thickness, load carried by oil film and surface asperities and non-dimensional squeeze film velocity are calculated for each cam angle degree.

On the other hand, to solve Dowson and Higginson formula, the summation of inertial force from valvetrain assembly and the valve spring load are calculated using equations (2.24) and (2.25) for each cam angle degree. Radius of curvature and the entraining velocity are derived from cam lift and used as an input in the oil film thickness formula.

Both Dowson and Higginson formula and Averaged Reynolds equations were solved simultaneously for every cam angle. According to the code algorithm, calculated minimum oil film thickness from Reynolds equation can not be smaller than Dowson and Higginson formula. Hence, some contact zones were found in hydrodynamic lubrication while some of them were found in EHD lubrication.

3. RESULTS AND DISCUSSION

3.1 Input Data Set

The input data for the analysis of the sample direct acting cam follower mechanism are listed in Table 3.1

Table 3.1 : Input Data

Parameter	Value
Base Circle Radius, m	18
Cam With, m	0.02
Valve Diameter, m	0.06
Valve Assembly Mass, kg	0.1
Clearance between Cam and Tappet, m	$20 * 10^{-6}$
Cam Surface RMS Roughness,m	$0.25 * 10^{-6}$
Tappet Surface RMS Roughness, m	$0.6 * 10^{-6}$
Composite Surface RMS Roughness, m	$0.65 * 10^{-6}$
Surface Pattern Parameter by Patir& Cheng	1
Cam - tappet Friction Coefficient	0.03
Cam - tappet Elastic Modulus, GPa	170
Cam - tappet Poisson's Ratio	0.28
Installed Spring Force, N	650
Lubricant Viscosity, Pa.s	0.014
Pressure Coefficient of Viscosity, 1/GPa	14.3
Camshaft Running Speed, rpm	1000

Calculated radius of curvature and hydrodynamic velocity curves are presented accordingly. These parameters are the main inputs for analyses. Figure 3.1 illustrates the variation in the radius of curvature as a function of cam angle. As can be seen from Figure 3.1 that while radius of curvature seems constant at the base circle zone of cam, it gets higher values at the flank zone of cam. The minimum radius of curvature is obtained around the nose of cam.

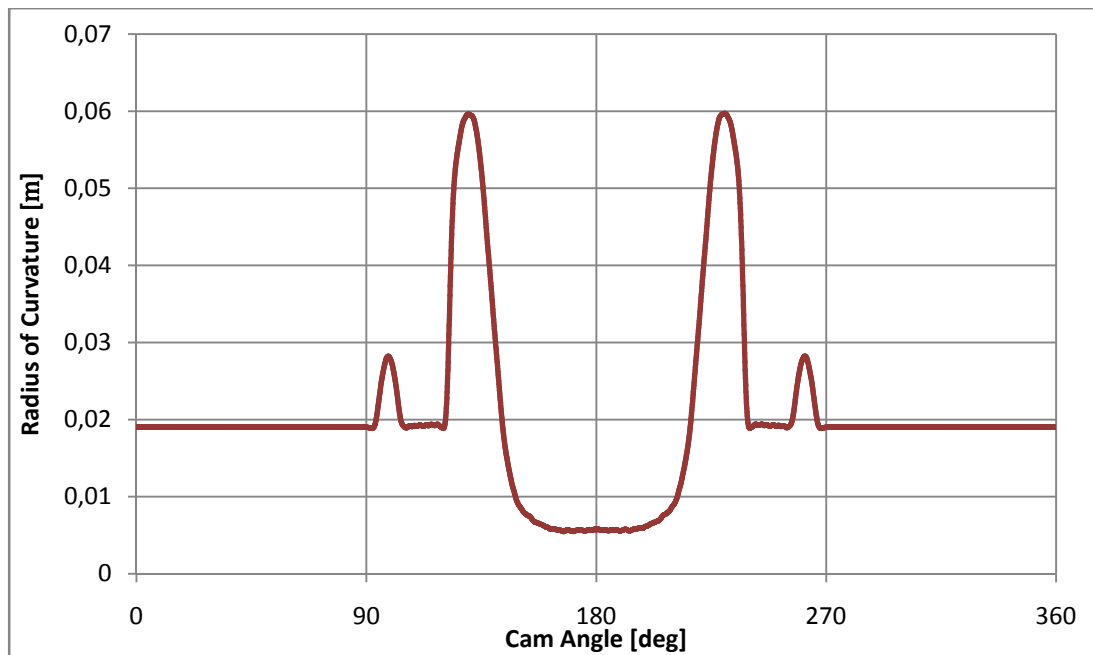


Figure 3.1 : Variation in the radius of curvature

Figure 3.2 shows the entraining velocity at 1000 rpm. Curve characteristic is similar to the radius of curvature because hydrodynamic velocity is derived from the radius of curvature formula. At the flank – nose transitions hydrodynamic velocities become zero. Theoretically, elastohydrodynamic oil film thickness is expected to be zero at these points, since the squeeze film effect is not considered in Dowson and Higginson's EHD model.

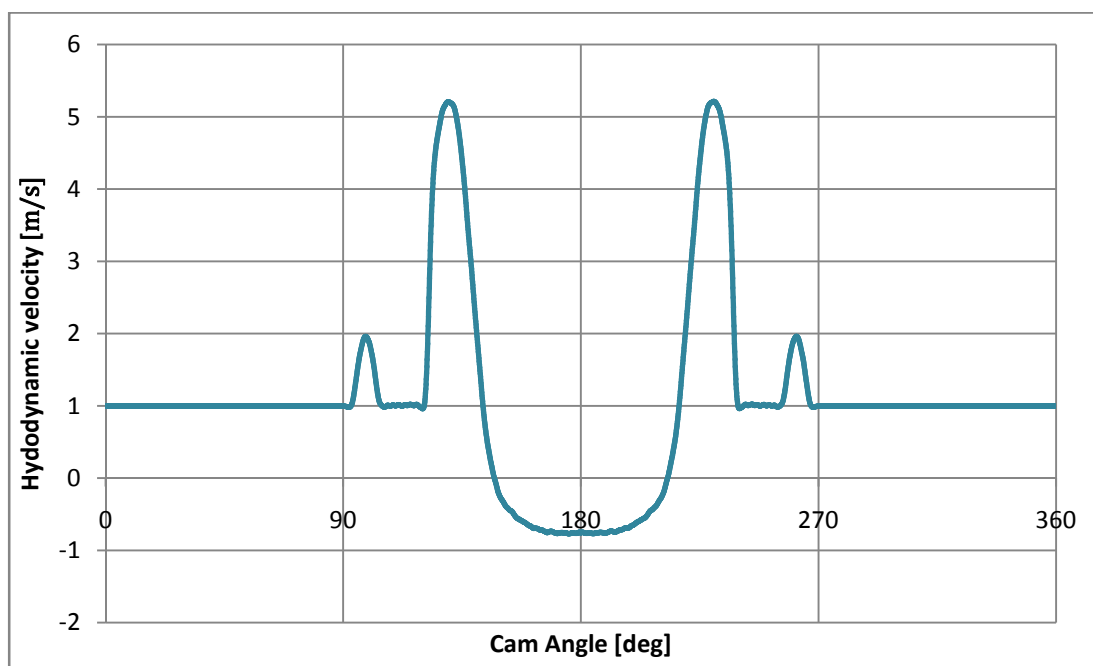


Figure 3.2 : Variation in the hydrodynamic velocity

3.2 Analysis Results

3.2.1 Effect of surface kinematics

Figure 3.1 shows the representative oil film thickness profile on the cam surface. In order to plot very small film thickness results on the cam surface, results are geometrically scaled.

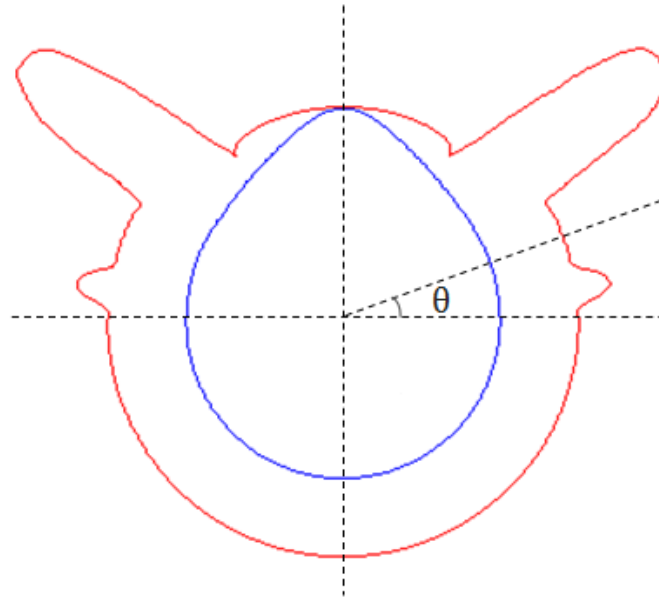


Figure 3.3 : Geometrically scaled oil film thickness profile

As can be seen from the plot above, oil film thickness changes dramatically at the flank zones of the cam. It is mainly caused by high radius of curvature at flank transitions. Oil film thickness reduces towards the cam nose, because of the small radius of curvature. Oil film remains constant at the rest of the cam surfaces, since the velocity and radius of curvature do not change at base circle zone.

Since cam surface can be divided into different geometric regions as a function of rotational angle, analysis results are examined according to defined cam zones. Figure 3.2 shows the oil film thickness at the cam - tappet interface.

The Base Circle: Between cam angle $\theta = 240$ and $\theta = 120$ stationary oil film thickness solution is obtained by using equation (2.1). Radius of curvature and entraining velocity of lubricant are lower compared to cam flank zone. Two small peaks at the oil film thickness curve are caused by hydrodynamic velocity changes before the cam flank zones. As a result of these parameters, elastohydrodynamic

behaviour is occurred between cam and tappet. Minimum oil film thickness is around $0.1 \mu\text{m}$.

The Flank: Between cam angle $\theta = 120 - 140$ and $\theta = 220 - 240$ hydrodynamic film formation is observed. Due to high radius of curvature and entraining lubricant velocity, Averaged Reynolds equation is solved. Both hydrodynamic and asperity pressures are obtained. This region is also called as the mixed lubrication region. Minimum oil film thickness reaches up to $0.5 \mu\text{m}$ at the middle of flank.

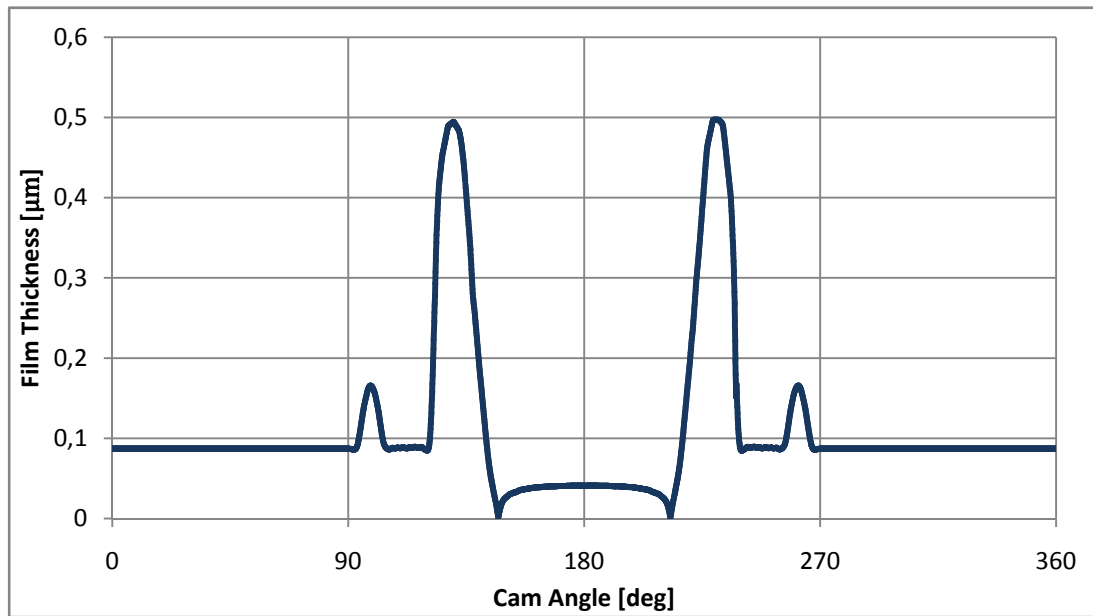


Figure 3.4 : Oil film thickness at the cam - tappet interface

The Nose: Between cam angle $\theta = 140$ and $\theta = 220$ elastohydrodynamic solution takes place again due to very small radius of curvature and very low entraining velocity. At a certain cam angle, the entraining lubricant velocity becomes zero then increases in the inverse direction. According the formula (2.1) oil film thickness is calculated zero where the entraining velocity is zero. However, due to the squeeze film effect, a small amount of lubricant remains between cam nose and tappet (Messe et al. 1999). Apart from the zero oil film thickness results, the film thickness obtained at the cam nose is around $0.04 \mu\text{m}$.

3.2.2 Effect of rotational speed

Various analyses are performed to investigate some of important parameters on the oil film thickness between cam and tappet. One of these parameters is the rotational cam speed. Cam speed is always defined as the half of crankshaft speed for 4 stroke internal combustion engines. Lubrication analyses are carried out in full speed range of one of conventional medium duty ICE. Figure 3.3 shows the oil film thickness at the cam - tappet interface for different engine speeds.

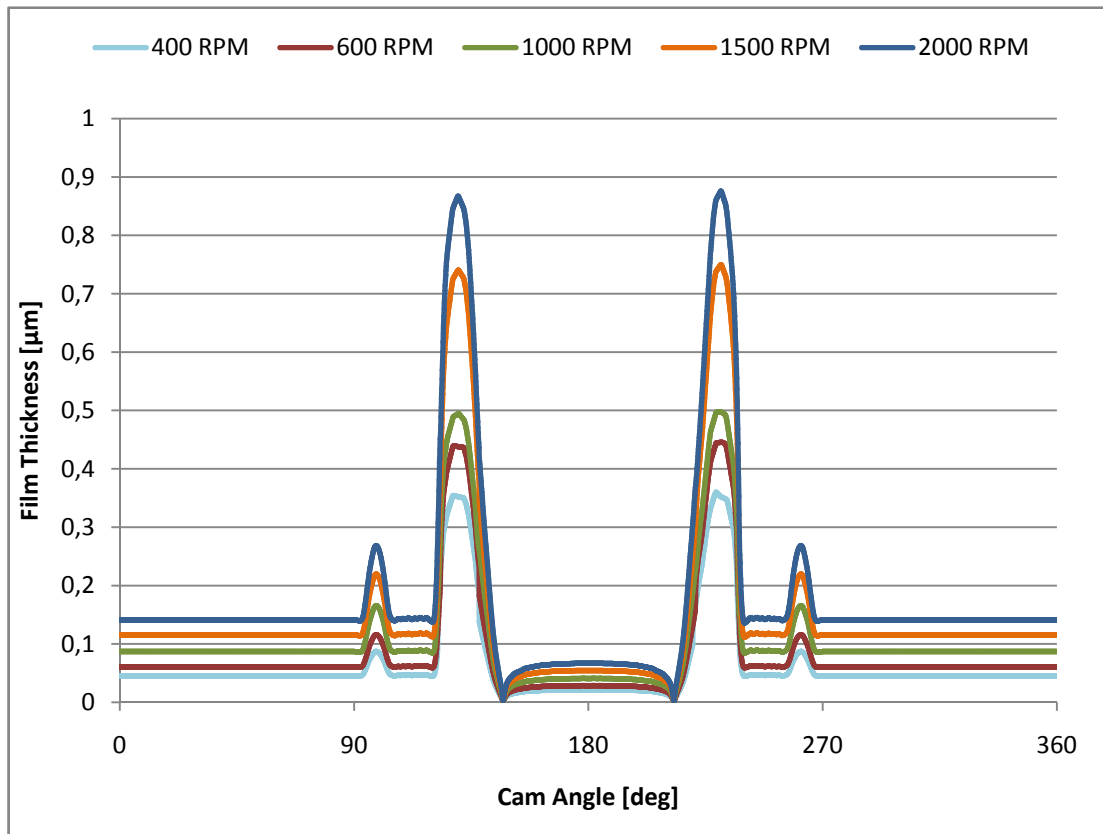


Figure 3.5 : Oil film thickness with different engine speeds

According to the analysis results, which are plotted above, oil film thickness increases with the higher engine speed. High rotational speed affects the entraining velocity. Thus, oil film thickness trend at cam - tappet interface depends on camshaft rotational speed directly. At the lowest engine running speed 400 rpm, oil film thickness decreases down to 0.01 µm around the cam nose. For the high engine speeds, oil film thickness reaches up to 0.9 µm around the cam flank. As indicated in previous statements, squeeze film effect prevents lubricant film thickness from collapsing even at the lowest engine speed.

3.2.3 Effect of lubricant viscosity

One of the other parameter that affects the oil film thickness is the lubricant dynamic viscosity. Various analyses are carried out under constant engine speed (1000 rpm) and constant operating temperature (70°C). Three different engine oils are selected and analyses are performed with their constant viscosity values. Figure 3.4 illustrates the oil film thickness results for three different types of oil; SAE 20, SAE 30, SAE 40.

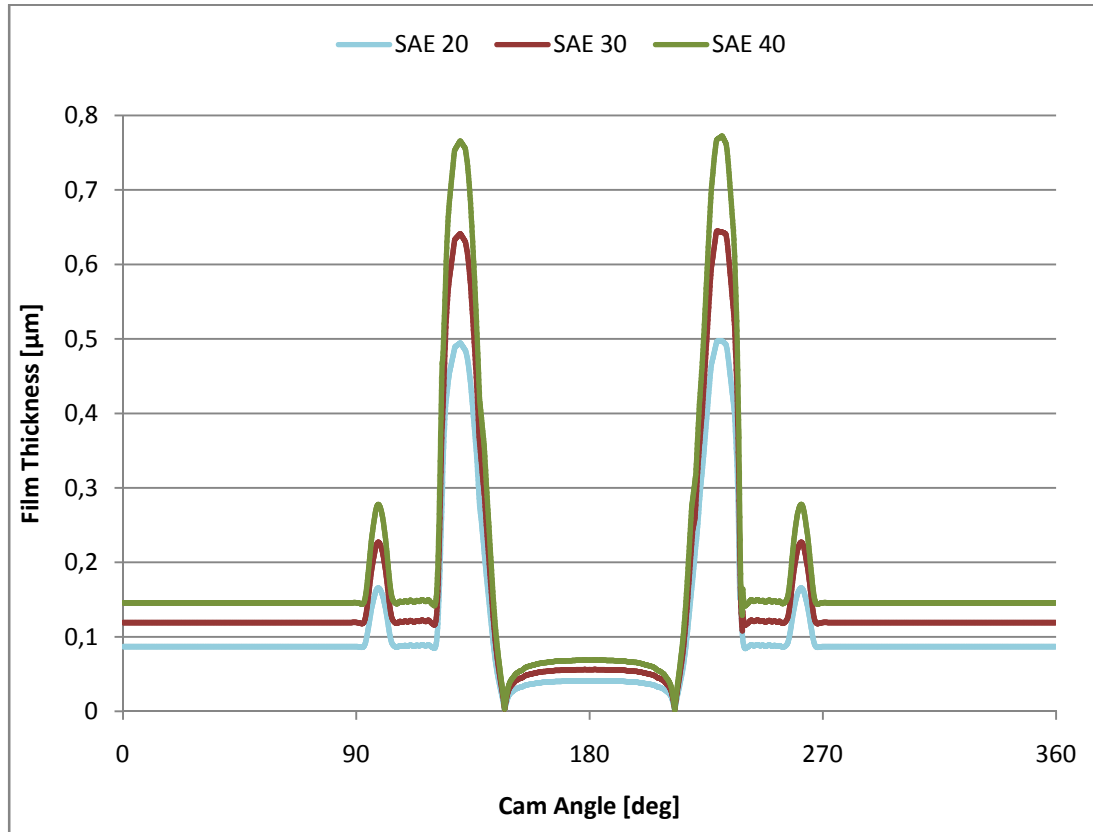


Figure 3.6 : Oil film thickness with various SAE grade oils

As the grade of oil increases, oil film thickness increases too. SAE 20 grade oil has 0.014 Pa.s and SAE 40 grade oil has nearly double of SAE 40's viscosity. The difference between the dynamic viscosities can be seen directly at film thickness results.

3.2.4 Comparison of classical EHD theory and developed calculation model

Oil film thickness profiles are calculated both with Dowson and Higginson formula and developed calculation model. Figure 3.5 shows the lubricant film thickness results, which are calculated with classical EHD theory and developed model.

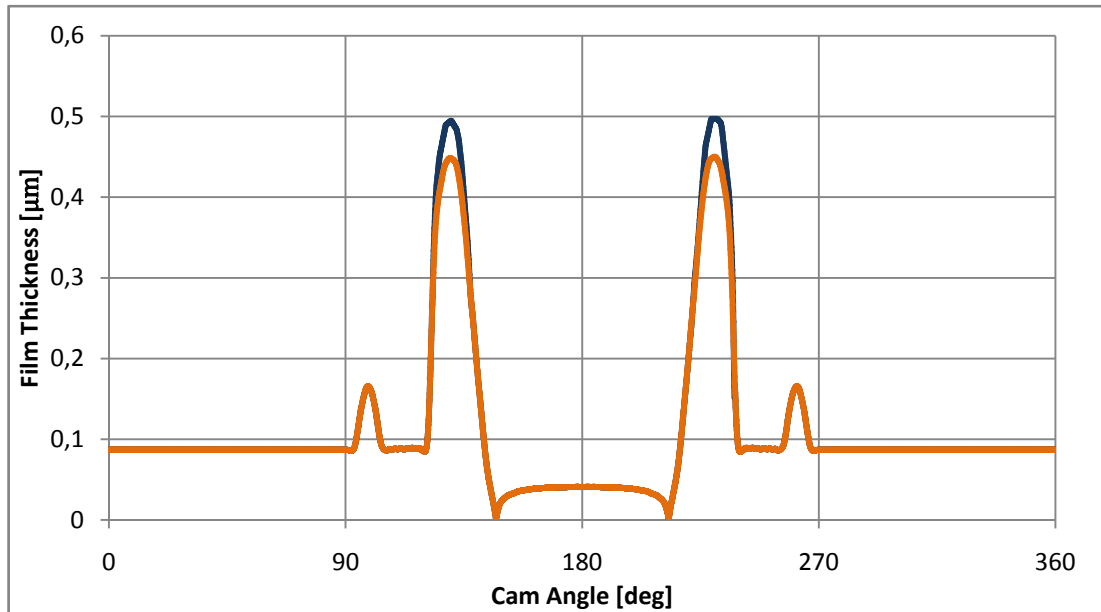


Figure 3.7 : Oil film thickness with classical EHD theory and developed model

There is no difference at the stationary part (Cam Base Circle) and cam nose part. The difference takes part at the cam flank zones. According to developed calculation model, hydrodynamic film formation occurs at flank zone. Thus, the lubricant thickness values are higher than calculated elasto hydrodynamic lubricant thickness values. At this region, transient term play an important role in order to calculate film thickness.

4. CONCLUSIONS

In order to assess cam - tappet lubrication performance, a new methodology has been developed. The methodology includes both elastohydrodynamic and mixed lubrication concepts. Variation in the load, the radius of curvature and the hydrodynamic entraining velocity are considered in the analysis. For the hydrodynamic lubrication regime, surface roughness characteristics are taken into account. By using developed calculation tool, any kind of cam - tappet design can be assessed in term of their lubrication performance. The model also can predict the effects of lubricant properties (i.e. lubricant viscosity) and contacting material properties (elastic modulus of materials). The model is expected to be beneficial for understanding of the dynamics of such complex cam - tappet systems.

In order to improve the model, deformation of the contacting surfaces can be included in the model. Thus, elastohydrodynamic lubrication regime can be solved instantaneously. Developed calculation model can also be extended by including crown radius and taper angle effects on the lubrication regime. Using the output of developed tool, friction coefficient determination and wear mechanism of cam - tappet interface can also be examined as a future work.

REFERENCES

- Akalin, O.**(1999). Piston ring and cylinder bore friction simulation in mixed lubrication regime. *PhD Thesis*, Wayne State University, Detroit, MI.
- Chang, L.** (1988). Numerical analysis of transient, line-contact problems in elastohydrodynamic lubrication,*PhD Thesis*,University of Illionis at Urbana-Champaign.
- Dowson, D.and Higginson, G. R.** (1966).Elasto-Hydrodynamic Lubrication, 236 pp., Pergamon, Oxford.
- Gecim, B. A.,** (1992). Tribological study for a low-friction cam/tappet system including tappet spin,*Tribology Transactions*,35:2, 225-234.
- Glovnea, R. P., and Spikes, H.A.**(2001).The Influence of Cam-Follower Motion on Eiaستohydrodynamic Film Thickness,*Tribology Research*, Elsevier Science B.V.
- Greenwood, J. A., and Tripp, J.H.**(1971).The Contact of Two Nominally Flat Rough Surfaces,*Proc. Inst. Mech. Eng.*, 185, pp. 625-633.
- Guangteng, G., Cann, P.M., Olver, A. V., Spikes, H.A.**(2000). An experimental study of film thickness between rough surfaces in EHD contacts,*Tribology International*, 33, 183-189.
- HookeC.J.**(1992).The Minimum Film Thickness in Lubricated Line Contacts during a Reversal of Entrainment,*Journal of Mechanical Engineering Scienc*,1992 206:417.
- Jiang, X., Hua, D. Y., Cheng, H. S., Ai, X. and Lee, S. C.** (1999).A mixed elastohydrodynamic lubrication model with asperity contact.*Journal of Engineering Tribology*, 121:481.
- Kreuter, P., and Pischinder, F.** (1985).Valve Train Calculation Model with Regard to Oil Film Effects, *SAE International Congress & Exposition*,Detroit, Michigan, February 25 – March 1.
- Kushwaha, M., Rahnejat, H., Jin, Z. M.**(2000).Valve-Ttrain Dynamics A Simplified Ttribo-Elasto-Multi-Body Analysis, *Journal of Multi-Body Dynamics*sp. 2000 214:95
- Kushwahu, M.** (2003).Tribological issues in cam-tappet contacts, in *Tribology and dynamics of engine and powertrain*p. 545-566, Woodhead Publishing Limited.
- Lee, K. M.**(1971). The Transient Solutions Of Elastohydrodynamic Lubrication,*PhD Thesis*, Northwestern University.
- Lubrecht, A. A.**(1987). The numerical solution of the elastohydrodynamically lubricated line and point contact problem, using multigrid techniques,*PhD Thesis*.

- Messe, S., and Lubrecht, A. A.** (2000). Transient elastohydrodynamic analysis of an overhead cam/tappet contact, *Journal of Engineering Tribology*, 214:415.
- Patir, N., and Cheng, H. S.** (1978). An Average Flow Model for Determining Effects of Three-Dimensional Roughness on Partial Hydrodynamic Lubrication, *ASME J. Lubr. Technology*, 100, pp. 12-17.
- Patir, N., and Cheng, H. S.** (1979). Application of Average Flow Model to Lubrication Between Rough Sliding Surfaces, *ASME J. Lubr. Technology*, 101, pp. 220-230.
- Robert L., and Norton, P. E.** (2002). Cam Design and Manufacturing Handbook, Industrial Press, Inc. 200 Madison Avenue New York.
- Roshan, R., Priest, M., Neville, A., Morina, A., Xia X., Green, J. H., Warrens, C. P., and Payne M. J.** (2009). Friction modelling in an engine valve train considering the sensitivity to lubricant formulation, *Journal of Engineering Tribology*, 223:413.
- Teodorescu, M., Taraza, D. and Henein, N. A.** (2003). Simplified elastohydrodynamic friction model of the cam-tappet contact, *SAE World Congress*, Detroit, Michigan, March 3-6.
- Teodorescu, M., and Taraza, D.** (2004). Combined multi-body dynamics and experimental investigation for determination of the cam-flat tappet contact condition, *Journal of Engineering Tribology*, 218:133.
- Taylor, C. M.** (1994). Fluid film lubrication in automobile valve trains, *Journal of Engineering Tribology*, 208:221.
- Vela, D., Ciulli, E., Piccigallo, B., and Fazzolari, F.** (2011). Investigation on cam-follower lubricated contacts, *Journal of Engineering Tribology*, 225:379.
- Wu, C., and Zheng, L.** (1989). An Average Reynolds Equation for Partial Film Lubrication With a Contact Factor, *ASME Journal of Tribology*, 111, pp. 188-191.
- Zhu, D.** (2007). On some aspects of numerical solutions of thin-film and mixed elastohydrodynamic lubrication, *Journal of Engineering Tribology*, 221:561.

CURRICULUM VITAE

Name Surname:Özgür Göçmen

Place and Date of Birth: İstanbul 1988

E-Mail: gocmenoz@itu.edu.tr

B.Sc.:I.T.U'2010 Mechanical Engineering

